Sonochemical Oxidation of Multiwalled Carbon Nanotubes

Yangchuan Xing,*,† Liang Li,† Charles C. Chusuei,*,‡ and Robert V. Hull‡

Departments of Chemical & Biological Engineering and Chemistry, University of Missouri—Rolla, Rolla, Missouri 65409-0010

Received November 5, 2004. In Final Form: March 7, 2005

Functionalization of carbon nanotubes (CNTs) is important for enhancing deposition of metal nanoparticles in the fabrication of supported catalysts. A facile approach for oxidizing CNTs is presented using a sonochemical method to promote the density of surface functional groups. This was successfully employed in a previous study [*J. Phys. Chem. B* **2004**, *108*, 19255] to prepare highly dispersed, high-loading Pt nanoparticles on CNTs as fuel cell catalysts. X-ray photoelectron spectroscopy (XPS), transmission electron microscopy, cyclic voltammetry, and settling speeds were used to characterize the degree of surface functionalization and coverage. The sonochemical method effectively functionalized the CNTs. A mixture of —C—O—/—C=O and —COO— was observed along with evidence for weakly bound CO at longer treatment times. The integrated XPS C 1s core level peak area ratios of the oxidized-to-graphitic C oxidation states, as well as the atom % oxygen from the O 1s level, showed an increase in peak intensity (attributed to $-CO_x$) with increased sonication times from 1 to 8 h; the increase in C surface oxidation correlated well with the measured atom %. Most of the CNT surface oxidation occurred between 1 and 2 h. The sonochemically treated CNTs were also studied by cyclic voltammetry and settling experiments, and the results were consistent with the XPS observations.

Downloaded via UNIV OF MASSACHUSETTS AMHERST on January 6, 2023 at 14:12:00 (UTC).
See https://pubs.acs.org/sharingguidelines for options on how to legitimately share published articles.

Introduction

Carbon nanotubes (CNTs) have extraordinary electronic, thermal, and mechanical properties that make them useful materials for a variety of applications,[1,2] including heterogeneous catalyst supports,[3−9] separation membranes,[10,11] field emission devices,[12,13] nanocomposites,[14,15] gas storage materials,[16] and chemical and biological sensors.[17−20] In many of these applications, CNTs have to be surface functionalized.[21,22] For example, surface oxidization is necessary for depositing high-loading catalytic metal nanoparticles on them,[3−9] polymer functionalization is required to obtain better dispersion in CNT nanocomposites,[14,15] and the attachment of biomolecules is needed to fabricate CNT-based biosensors.[18]

Among various surface functionalization techniques, oxidation is probably the most widely studied. Oxidation of raw CNTs has been used to remove amorphous carbon for purification purposes[23−25] and to open CNT ends for metal nanoparticle insertion.[26,27] Early treatment techniques have involved gas-phase oxidation in air and oxidative plasmas,[23] but these techniques have led to an over-oxidation of CNTs, often removing or severely damaging the CNTs in addition to removing the amorphous carbon. A low yield of oxidized CNTs subsequently results. Liquid-phase oxidation involves acidic etching with nitric and/or sulfuric acids. Compared to gas-phase oxidation, liquid-phase oxidation (via HNO_3 and H_2SO_4) is mild and slow, and can provide a high yield of oxidized CNTs.[25] For amorphous carbon removal and end opening, oxidation damage to the surface of the CNTs is not desired.

* Corresponding authors. E-mail: xingy@umr.edu (Y.X.); chusuei@umr.edu (C.C.C.).

† Department of Chemical & Biological Engineering, University of Missouri—Rolla.

‡ Department of Chemistry, University of Missouri—Rolla.

(1) Harris, P. *Carbon Nanotubes and Related Structures: New Materials for the Twenty-First Century*; Cambridge University Press: New York, 2001.
(2) Dresselhaus, M. S.; Dresselhaus, G.; Avouris, P. *Carbon Nanotubes: Synthesis, Structure, Properties and Applications*; Springer-Verlag: New York, 2001.
(3) Planeix, J. M.; Coustel, N.; Coq, B.; Brotons, V.; Kamblar, P. S.; Dutartre, R.; Geneste, P.; Bernier, P.; Ajayan, P. M. *J. Am. Chem. Soc.* **1994**, *116*, 7935.
(4) Freemantle, M. *Chem. Eng. News* **1996**, *74*, 62.
(5) Che, G.; Lakshmi, B. B.; Fisher, E. R.; Martin, C. R. *Nature* **1998**, *393*, 346.
(6) Che, G.; Lakshmi, B. B.; Martin, C. R.; Fisher, E. R. *Langmuir* **1999**, *15*, 750.
(7) Li, W.; Liang, C.; Qiu, J.; Zhou, W.; Han, H.; Wei, Z.; Sun, G.; Xin, Q. *Carbon* **2002**, *40*, 791.
(8) Yoshitake, T.; Shimakawa, S.; Kimura, H.; Ichihashi, T.; Kubo, Y.; Kasuya, D.; Yakahashi, K.; Kokai, F.; Yudasaka, M.; Iijima, S. *Physica B* **2002**, *323*, 124.
(9) Gennett, T.; Landi, B. J.; Elich, J. M.; Jones, K. M.; Alleman, J. L.; Lamarre, P.; Morris, R. S.; Raffaelle, R. P.; Heben, M. J. *Mater. Res. Soc. Symp. Proc.* **2003**, *756*, 379.
(10) Sun, L.; Crooks, R. M. *J. Am. Chem. Soc.* **2000**, *122*, 12340.
(11) Zhang, L.; Melechko, A. V.; Merkulov, V. I.; Guillorn, M. A.; Simpson, M. L.; Lowndes, D. H.; Doktycz, M. J. *Appl. Phys. Lett.* **2002**, *81*, 135.
(12) Bonard, J.-M.; Weiss, N.; Kind, H.; Stocki, T.; Forro, L.; Kern, K.; Chatelain, A. *Adv. Mater.* **2001**, *13*, 184.
(13) Sugino, T.; Yamamoto, T.; Kimura, C.; Murakami, H.; Hirakawa, M. *Appl. Phys. Lett.* **2002**, *80*, 3808.
(14) Ajayan, P. M.; Schadler, L. S.; Giannaris, C.; Rubio, A. *Adv. Mater.* **2000**, *12*, 750.
(15) Rossi, G. B.; Beaucage, G.; Dang, T. D.; Vaia, R. A. *Nano Lett.* **2002**, *2*, 319.
(16) Schlapbach, L.; Zuttel, A. *Nature* **2001**, *414*, 353.
(17) Sherigara, B. S.; Kutner, W.; D'Souza, F. *Electroanal.* **2003**, *15*, 253.
(18) Zhang, Y.; Li, J.; Shen, Y.; Wang, M.; Li, J. *J. Phys. Chem. B* **2004**, *108*, 15343.
(19) Poh, W. C.; Loh, K. P.; Zhang, W. D.; Triparthy, S.; Ye, J.-S.; Sheu, F.-S. *Langmuir* **2004**, *20*, 5484.
(20) Valentini, F.; Orlanducci, S.; Terranova, M. L.; Amine, A.; Palleschi, G. *Sens. Actuators, B* **2004**, *100*, 117.
(21) Ebbesen, T. W.; Hiura, H.; Bisher, M. E.; Treacy, M. M. J.; Shreeve-Keyer, J. L.; Haushalter, R. C. *Adv. Mater.* **1996**, *8*, 155.
(22) Ros, T. G.; van Dillen, A. J.; Geus, J. W.; Koningsberger, D. C. *Chem.—Eur. J.* **2002**, *8*, 2868.
(23) Ebbesen, T. W.; Hiura, H.; Fujita, H.; Tanigaki, K. *Nature* **1994**, *367*, 519.
(24) Tsang, S. C.; Chen, Y. K.; Harris, P. J. F.; Green, M. L. H. *Nature* **1994**, *372*, 159.
(25) Hiura, H.; Ebbesen, T. W.; Tanigaki, K. *Adv. Mater.* **1995**, *7*, 275.
(26) Tsang, S. C.; Harris, P. J. F.; Green, M. L. H. *Nature* **1993**, *362*, 520.
(27) Ajayan, P. M.; Ebbesen, T. W.; Ichihashi, T.; Iijima, S.; Tanigaki, K.; Hiura, H. *Nature* **1993**, *362*, 522.

10.1021/la047268e CCC: $30.25 © 2005 American Chemical Society
Published on Web 04/02/2005

Samsung Ex. 1015, Page 1 of 6
Samsung Electronics Co., Ltd., et al. v. Molecular Rebar Design, LLC
IPR2025-00355

To use CNTs as heterogeneous catalyst supports, the entire surface of CNTs needs to be oxidized for functionalization so that highly dispersed catalysts could be achieved. Surface oxidation of CNTs for this purpose was generally approached using acidic reflux,[7,28] in which oxidative acids, such as nitric and sulfuric acids, were used with or without other oxidants. Acidic reflux processes need a prolonged oxidization period, often as long as 3 days for surface oxidation. Unfortunately, even with a prolonged treatment, refluxed CNTs failed to result in a uniform deposition of catalytic metal nanoparticles. The reason for this failure was attributed to the impartial surface oxidation of the CNTs.[29] Since CNTs have a hydrophobic surface, they tend to form aggregates in polar solvents. During the acidic reflux process, some CNTs inside these aggregates may not be attacked by the oxidative agents but remain unmodified.

In an effort to prepare highly dispersed, high-loading Pt nanoparticles on CNTs, a sonochemical technique was successfully employed for oxidation treatment of multiwalled CNTs.[29] Sonication was used for the entire treatment process to keep the CNTs dispersed. It was found that sonochemically treated CNTs resulted in the deposition of uniformly dispersed Pt nanoparticles. Despite this observation, the effects of sonication on the surface oxidation of CNTs were not characterized. We report here a detailed study of the sonochemical treatment with emphasis on its effects on morphological and surface structure. Particular attention is paid to delineating surface functional groups tethered to the CNT surface.

Experimental Methods

Oxidization of CNTs. The sonochemical treatment procedure is the same as reported previously,[29] except that the duration of treatment was varied in this study. Therefore, only a brief description of the procedure is given here. The CNTs used in this study (purchased from NanoLab, Inc.) are multiwalled CNTs synthesized from a chemical vapor deposition process. The as-purchased CNTs (95% purity, ~30 nm in diameter) were put into a mixture solution of HNO_3 and H_2SO_4 in an Erlenmeyer flask. The concentrations of both acids were 8.0 M. The flask was placed in an ultrasonic bath (Fisher Scientific, 130 W and 40 kHz) maintained at 60 °C. The treatment was performed for 1, 2, 4 and 8 h. The sonochemically treated CNTs were then separated from the acids in a centrifuge (Thermal IEC Centra CL2), and thoroughly washed using doubly distilled, deionized water prior to analysis.

Morphological Characterization. The morphology of the carbon nanotube was characterized using a high-resolution transmission electron microscope (TEM). The TEM (EM 430, Philips) was operated at 300 kV with 400-mesh carbon-coated copper TEM grids (Electron Microcopy Sciences, CF-400Cu). The sample preparation for the TEM is as follows. A small amount of the CNTs were dispersed in ethanol and a drop of the dispersion was taken and put on a TEM grid using a pipet. The drop on the grid was allowed to dry in the open atmosphere and the TEM grid was then examined. Images of the CNTs were obtained for morphological analysis.

Characterization of Dispersion and Surface Oxidation State. Treated and untreated CNTs were studied by measuring their settling speeds. A graduated 50 mL buret was filled with either deionized water or ethanol, followed by dropping concentrated CNT dispersion via a transfer pipet at the top of the buret. The distance traveled as the CNTs settled to the bottom of the buret (due to gravity), as a function of time, was measured to obtain the settling speed, which served as an indirect measurement of the degree of the surface functionalization.

X-ray photoelectron spectroscopy (XPS) measurements were performed on the CNTs in an ion-pumped Perkin-Elmer PHI ESCA 560 system using a PHI 25-270AR double pass cylindrical mirror analyzer (CMA). A Mg Kα anode, operated at 15 kV and 250 W with a photon energy of $h\nu = 1253.6$ eV, was used. The base pressure of the chamber after a bakeout was $\sim 1 \times 10^{-10}$ Torr. The operating pressure during the XPS scans was in a range that did not exceed 5×10^{-8} Torr. Samples were mounted onto a sample probe with double-sided tape (3M Scotch) and loaded into the main UHV analysis chamber via a turbopumped antechamber. The C 1s core level at 284.4 eV, corresponding with the CNT oxidation state,[30] was used to charge reference the XP spectra. The XPS data was curvefitted using CasaXPS VAMAS processing software version 2.2 (Devon, United Kingdom) with a Shirley background subtraction[31] and 70%-to-30% Gaussian−Lorentzian line shapes.

Cyclic voltammetry (CV) was used to study the surface oxide groups on the CNTs. Each sample of the CNTs was made into a paste in a water-ethanol (3:2 volume ratio) solution. In preparing the electrode, a 20 μL drop of the paste was put on a glassy carbon disk. After drying in a vacuum furnace, a drop of 5 wt % Nafion in water solution (Alfa Aesar) was spread onto the CNTs and allowed to dry to form a recast ionomer thin film. Electrochemical measurements were made using a potentiostat (Bioanalytical Sciences, BAS100) in deaerated 1.0 M H_2SO_4, with a rotating disk electrode scanned at 20 mV/s at room temperature at a rotating speed of 1000 rpm.

Results and Discussion

Figure 1 shows typical TEM images of the sonochemically treated CNTs at varied treatment times. After surface oxidation, the surface of the CNTs became heterogeneous due to the attack by the oxidative acids. TEM images showed that the surface morphology changed from a smooth surface of the original CNTs (not shown) to a rougher surface of the sonochemically treated CNTs. The treated CNTs can be seen to have an increase in surface roughness as a function of treatment time. The rough surface of treated CNTs was attributed to the acidic etching of the CNT surfaces. Both nitric and sulfuric acids can attack the CNT surfaces, though the etching process was found to be generally slow under reflux conditions.[25] With the assistance of sonication, the oxidation process was expedited as can be seen in the 8-h sample which had severe surface etching. Note that the treated CNTs did not show measurable changes in diameters and lengths when low magnification TEM images were examined. It has been shown previously that sonication can fragment the CNTs[25−27] and cause mechanical damage to their surface. The reason that we did not see such damages in our CNTs may be due to the fact that the ultrasonic bath we used had a low output power and the sonication time was not long enough. However, since the purpose of our work was to functionalize the CNT surface, damage of the original CNTs was not desired although the increased surface roughness was an indication of a denser population of surface functional groups.

The settling speeds, measured via the downward drift of the CNTs in a buret, correlated with a longer sonication time and, hence, higher surface functionalization. The increased settling speed was due to decreased interaction of the functional groups on the CNTs with the surrounding solvent. As the CNTs became more functionalized, the solvent-CNT interactions increased, leading to longer settling times. Therefore, as sonication times were increased, the settling speeds of the CNTs were decreased. The CNT settling speeds (with error bars) in water and ethanol are shown in Table 1, which were obtained from four measurements. The settling speeds in both solvents

(28) Lordi, V.; Yao, N.; Wei, J. *Chem. Mater.* **2001**, *13*, 733.
(29) Xing, Y. *J. Phys. Chem. B* **2004**, *108*, 19255.
(30) Suzuki, S.; Watanabe, Y.; Ogino, T.; Heun, S.; Gregoratti, L.; Barinov, A.; Kaulich, B.; Kikinova, M.; Zhu, W.; Bower, C.; Zhou, O. *Phys. Rev. B* **2002**, *66*, 035414.
(31) Shirley, D. A. *Phys. Rev. B* **1972**, *5*, 4

Samsung Ex. 1015, Page 2 of 6
Samsung Electronics Co., Ltd., et al. v. Molecular Rebar Design, LLC
IPR2025-00355

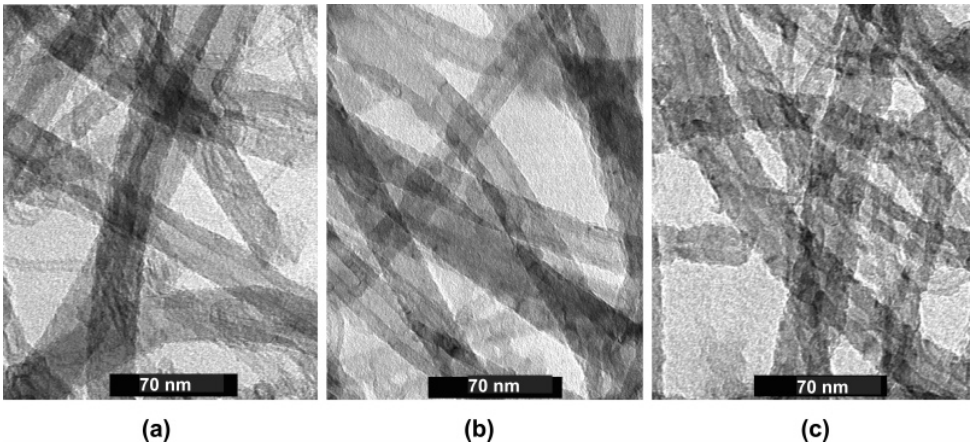

Figure 1. TEM Images of sonochemically-treated CNTs, showing the surface morphology changes at (a) 2 h, (b) 4 h, and (c) 8 h.

Table 1. Settling Speeds of Sonochemically Treated CNTs in Water and Ethanol

ultrasonic treatment time (hrs)	CNT settling speed (mm/min)	
	in water	in ethanol
none	33.7 ± 0.3	36.6 ± 0.4
1	19.8 ± 0.1	21.7 ± 0.3
2	15.2 ± 0.1	19.8 ± 0.4
4	12.1 ± 0.4	14.3 ± 0.3
8	3.2 ± 0.4	3.7 ± 0.3

were similar although the CNT settling speeds in ethanol were slightly faster than those in water probably because of decreased H-bonding.

Photographs of CNT settlings in test tubes were taken at various times for samples with different treatment durations, as shown in Figure 2. Initially, the CNTs were uniformly dispersed in water by a vortex mixer. The untreated CNTs formed large aggregates immediately after they were taken off the mixer, and began to settle. In contrast, the treated CNTs had better dispersion and took longer to settle, with the majority of the 8-h sample remaining dispersed in water throughout the experiment. Some of the CNTs in the 8-h sample remained in suspension (did not settle). The sample solution remained black, demonstrating that there were water "soluble" CNTs in the sample. XPS core level shifts offer further elucidation of the chemical oxidation states of the resulting, oxidized CNTs. A listing of the measured binding energies along with peak assignments referred to in Figures 3 and 4 are summarized in Table 2.

Figure 3 shows the C 1s core level photoemission spectra of sonochemically treated CNTs as a function of treatment time. For comparison, the spectrum obtained for the blank CNT (without treatment) is also shown. The untreated CNT shows a dominant peak structure for the C 1s core level at a binding energy (BE) of 284.4 eV, which corresponds to the bare, untreated CNT surface.[30,32] The peak has a slightly asymmetric line shape with a high binding energy tail. The C 1s line shapes changed with increased sonication time, corresponding to greater oxidation of the CNT surface (Figure 3). The broadening of the envelope is attributed to the functionalization of the surface with increasing treatment time. The core level shift of C1 is assigned to the graphitic carbon of the untreated CNTs;[30,32] peaks C2 and C3, resulting from the sonochemical functionalization, denote —C—O— (286.7 eV) and —COO— (288.3 eV) functional groups, respectively, and are in agreement with literature

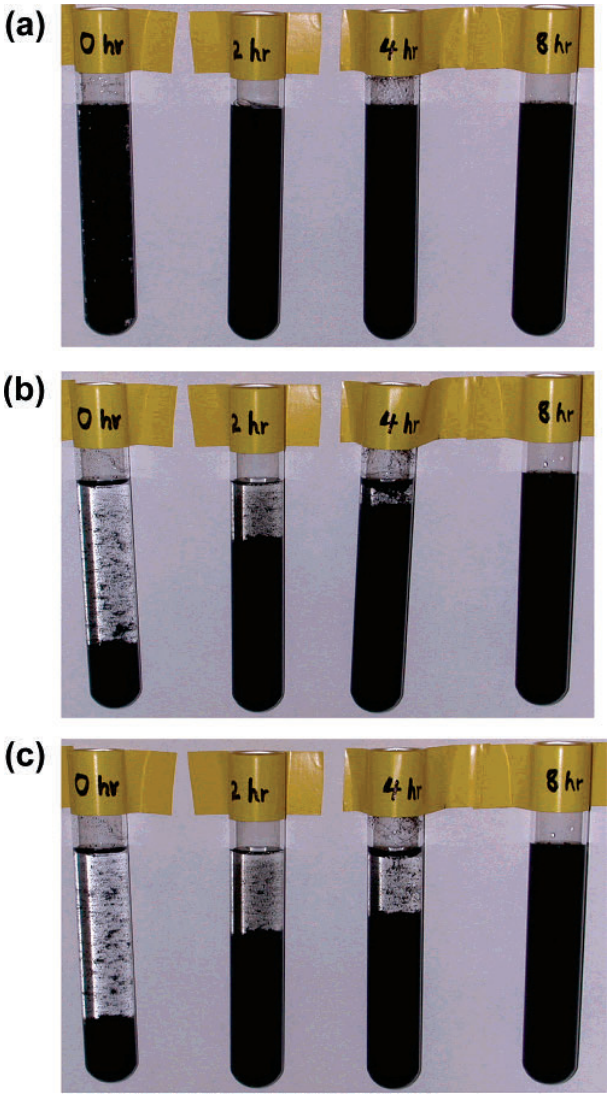

Figure 2. Photographs of CNTs drifting downward in test tubes for ultrasonication of 0, 2, 4, and 8 h (a) immediately after colloidal suspension perturbation, (b) 5 min after perturbation, and **(c)** 10 min after perturbation.

(32) Ago, H.; Kugler, T.; Franco, C.; Salaneck, W. R.; Shaffer, M., S. P.; Windle, A. H.; Friend, R. H. *J. Phys. Chem. B* **1999**, *103*, 8116.

Samsung Ex. 1015, Page 3 of 6
Samsung Electronics Co., Ltd., et al. v. Molecular Rebar Design, LLC
IPR2025-00355

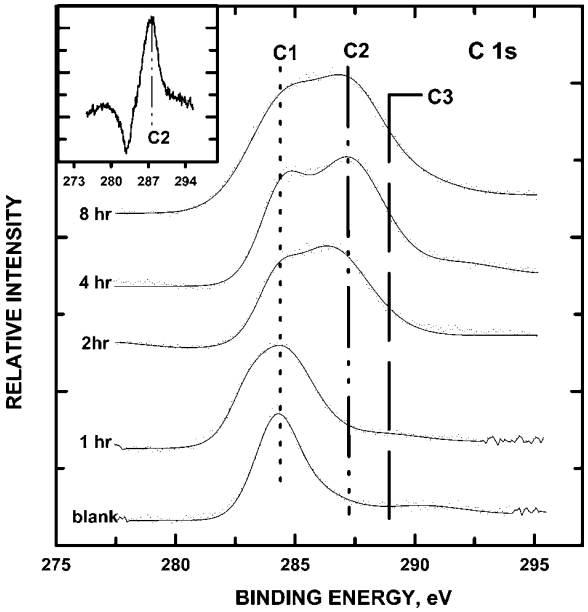

Figure 3. XPS stackplot of C 1s core level of the CNTs at varying sonochemical treatment times. The inset shows the difference spectrum of the 4 h minus 1 h CNT treatment; peak C2 is pronounced.

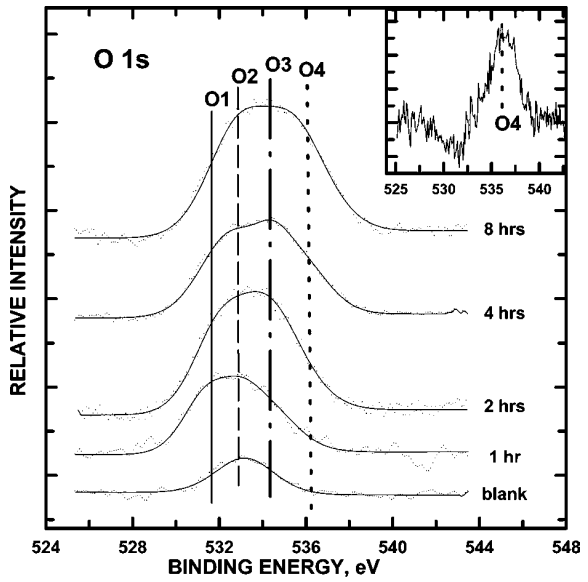

Figure 4. XPS stackplot of O 1s core level of the CNTs at varying sonochemical treatment times. The inset shows the difference spectrum of the 8 h minus 2 h CNT treatment; peak O4 is pronounced.

these groups tethered onto the CNTs.[25] A marked increase in the surface population of —C—O— is evident (C2), while the addition of —COO— (C3) is small. Previous studies have reported a —C=O species at 287.6 eV.[33−35] Intensity at this BE position is evident in the C 1s stackplot (Figure 3) after 2 h of sonochemical treatment and beyond. However, given the resolution of the C 1s spectra (between ~2.0−3.0 eV), it is difficult to deconvolute contributions from —C=O; adding an additional peak would over interpret the data. The quantitative details of the —C=O were lost in the C 1s spectra due to large contributions from —C—O—. However, quantitation of the —C=O groups is possible from the O 1s spectra (*vide infra*). Noting the observed trends in the C 1s spectra, we postulate that the increased density of the Pt nanoparticle formation in our earlier procedure[29] was predominantly attributed to interactions with —C—O— that formed. The relatively low intensity at the —COOH position suggests that, by the 2−4 h CNT treatment time, —C—O—/—C=O functionality, and not —COOH, plays a major role in the successful deposition of the metallic nanoparticles. The relatively low intensity of peak C3 and high intensity of peak C2 as a function of treatment time show that the CNTs were oxidized with the carbon bonded to more oxygen as the treatment process progresses. The —COOH component showed no appreciable increase with increased treatment time. Note that intensities between 288 and 289 eV in the C 1s difference spectrum and subtracting counts between the 1st and 4th hour experiments show diminished intensity at the —COO— BE location. In contrast, the C 1s difference spectrum (inset of Figure 3) shows intensity at ~287 eV, consistent with —C—O— functionality present during the Pt cluster decoration. The ~ +3 eV chemical shift of peak C2, relative to unoxidized carbon at 284.4 eV, denotes an increased net positive charge on the carbon atom, an effect that is typically pronounced in oxidation processes.[36] Peak C2 is the dominant oxidation state (denoting —C—O—) after 2 h of treatment. Peak C3 is dwarfed by peak C2 as indicated by low intensity in the difference spectrum (inset in Figure 3). The C 1s line broadening with extra feature developments are attributed to the surface oxidation of CNT where C atoms bond to more O atoms as a result of the sonochemical treatment. The marked differences in the XPS C 1s line shapes for 1- and 2-h sonication times denote the most rapid —C—O—/—C=O generation rate where much of the surface oxidation occurred. A leveling off of the surface functionalization was observed at 4−8 h, more pronounced in the plot of surface oxygen content versus treatment time, which is likely due to the limitation of the low ultrasonic bath power (130 W).

The O 1s stackplot (Figure 4) follows the same trend. An additional piece of information, not available in the C 1s stackplot is the development of the —C=O and —C—O— functional groups at O 1s BE = 531.3 and 533.0 eV, respectively, which was also observed by other groups[35,37] in their analysis of oxidized CNTs. Fortunately, this feature is more visible since it is at the lowest BE peak

Table 2. Summary of XPS Peak Assignments of the Chemical Oxidation States of Sonochemically Treated CNTs of the O 1s and C 1s Core Levels[a]

peak	BE, eV	fwhm, eV	assignment
O1	531.3	2.5	—C=O
O2	533.0	2.3	—C—O—
O3	534.4	3.0	—O—COO—, H_2O
O4	536.5	3.1	adsorbed CO
C1	284.4	3.2	graphitic C
C2	286.7	2.3	—C—O—
C3	288.3	3.0	—COO—

[a] Peak centers and full widths at half-maxima (fwhm) were based on curve-fitting the 8-h sonochemically treated CNTs.

(33) Hidefumi, H.; Ebbeson, T. W.; Katsumi, T. *Adv. Mater.* **1995**, *7*, 275.
(34) Lee, W. H.; Lee, J. G.; Reucroft, P. J. *Appl. Surf. Sci.* **2001**, *171*, 136.
(35) Martinez, M. T.; Callejas, M. A.; Benito, A. M.; Cochet, M.; Seeger, T.; Anson, A.; Schreiber, J.; Gordon, C.; Marhic, C.; Chauvet, O.; Fierro, J. L. G.; Maser, W. K. *Carbon* **2003**, *41*, 2247.
(36) Brundle, C. R.; Baker, A. D. *Electron Spectroscopy: Theory, Techniques and Applications*; Academic Press: London, 1984.
(37) Hontora-Lucas, C.; Lopez-Peinado, A. J.; Lopez-Gonzalez, J. D.; Rojas-Cervantes, M. L.; Martin-Aranda, R. M

Samsung Ex. 1015, Page 4 of 6
Samsung Electronics Co., Ltd., et al. v. Molecular Rebar Design, LLC
IPR2025-00355

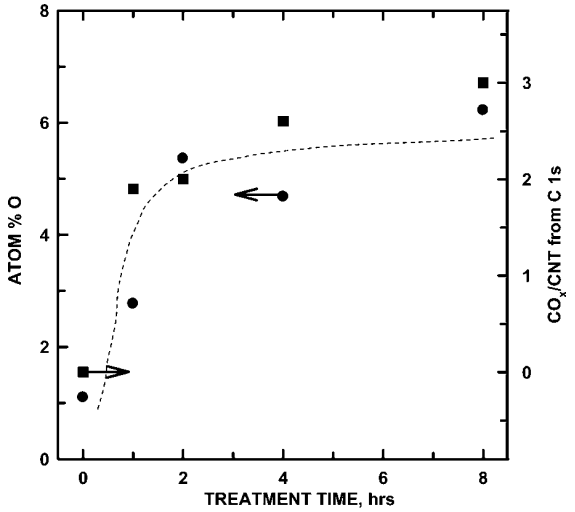

Figure 5. Uptake plot of the oxidized-to-graphitic carbon, CO_x/CNT (■; right axis) and atom % oxygen (●; left axis) of sonochemically treated CNTs as a function of the treatment time. The dashed line serves as a guide to the eye for the trend of atom % oxygen.

(O1) in this stackplot data set. The relatively small signal (as compared to the other chemical oxidation state assignments) denotes a relatively small population of —C=O. Note that even in the blank CNT, residual —C—O— is present on the CNT, as denoted by peak at 533.0 eV. After the first hour of sonochemical treatment, peaks attributed to the —C=O and —C—O— quickly began to develop. This development is also supported by the C 1s stackplot data. Note that C3 (Figure 3) increases, but does not contribute appreciably in the C 1s difference spectrum. Instead, C2, attributed to —C—O—, dominates. At 2 h, peak O3, which we assign to —C—OO— on the surface,[38] appears and dominates in the 2- to 8-h treatment times. For O 1s BE = 534.3 eV, the —O—COO— group has been reported for polyvinylenecarbonate adsorbed onto graphite surfaces.[38] There may be contributions from adsorbed H_2O in the O3 peak intensity resulting from exposures to aqueous solution, which was also seen by Martinez et al.[35] in their CNT oxidation study. The overlap of the chemical shifts makes it difficult to distinguish between H_2O and —C—OO— from these data alone. Future vibrational studies would shed light on this aspect. Finally, peak O4 appears between 4-to-8 h of sonication. Peak O4 was evident in the difference spectrum between the 8-h and 2-h experiments. The origin of the feature at O4 is unclear, but may be indicative of loosely bound —C=O. Carbon monoxide fragmentation from laser-ablated poly(ethylene terephthalate) has been known to produce CO fragments at characteristic O BEs = 536.4 eV.[39] The origin of the O4 signal may be the result of fragmentation of the tethered —COO— groups. The decomposition and/or fragmentation of this group could result in loosely bound CO, and hence signal at O4.

The population of the oxidized groups (—C—O—/—C=O/—COO—) relative to the CNT carbon can be quantified via plotting the sum of their C 1s peak areas relative to that of the graphitic CNT carbon as a function of sonochemical treatment time (Figure 5). The increase in surface oxidation as a measure of the relative amounts of oxidized carbon (CO_x) to the CNT tracks well with the overall O content measured by the XPS atom %. The trends in increased CNT oxidation measured by both the atom % O and relative CO_x/CNT intensities from the C 1s level are in good agreement with one another. A greater uptake of oxygen by the surface carbon atoms corresponds to a higher population density of CO_x functional groups as detected by the XPS. Notable differences in oxygen uptake (noteworthy at the 1- and 4-h treatment times) can be attributed to varying amounts of physisorbed O, which is detectable in the O 1s but not in the C 1s spectra. The high BE features in the C 1s spectra (C2 and C3) are due to chemically bonded O in the CNT structure. The O 1s signal, on the other hand, does not distinguish between chemi- and physisorbed oxygen; contributions from both interactions appear in the signal (Figure 4). From the uptake curves (of both the at. % O and CO_x/CNT relative intensities), it is evident that the surface oxidation of CNT stabilized at 2−4 h with oxidative saturation reached at 4 h. Corroborating with the results of the individual C 1s and O 1s stackplots, much of the CNT surface oxidation activity seemed to occur within 1−2 h, as indicated by the dashed line in Figure 5.

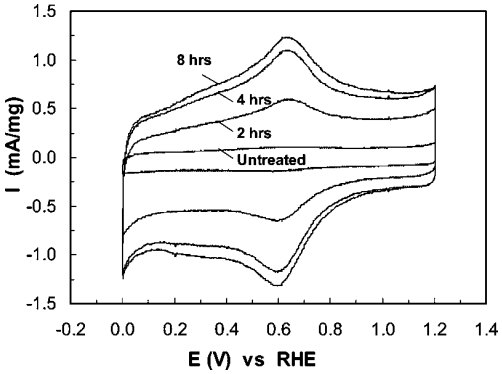

Figure 6. Cyclic voltammograms of the sonochemically treated CNTs obtained in 1.0 M H_2SO_4. The CV of untreated CNTs is also displayed for comparison. The increase in peak current corresponds to the increased treatment time. Voltage scan rate = 20 mV/s; electrode rotation speed = 1000 rpm.

Figure 6 displays the CV results of the CNTs. The voltammograms show anodic peaks at ~ 0.64 V and cathodic peaks at ~0.58 V for the treated CNTs that were associated with the oxidation and reduction of the surface oxide groups. The blank sample shows no evidence of oxidation and reduction of the surface oxides, indicating that the original CNTs had few surface oxide groups; the constant current in the potential region is attributed to double layer charging. The capacitance of this double layer is estimated to be ~6.0 F/g, comparable to that of graphitized carbon black (~5.6 F/g).[40] The heights of the redox peaks of the sonochemically treated CNTs, shown in Figure 6, increased with longer treatment times, suggesting that longer times produced more surface oxide groups. Although the exact number of surface groups cannot be determined due to an incomplete definition of surface redox reactions, the relative amounts can be roughly estimated from the peak currents. The ratio of the specific cathodic current of the 4-h sample to that of the 2-h sample was calculated to be 1.81. However, a smaller ratio of 1.12 for the 8-h to the 4-h sample was obtained, demonstrating that a saturation of the surface functional groups was reached, in agreement with the XPS results.

(38) Ota, H.; Sakata, Y.; Inoue, A.; Yamaguchi, S. *J. Electrochem. Soc.* **2004**, *151*, A1659.
(39) Watanabe, H.; Yamamoto, M. *J. Polym. Sci.* **1997**, *64*, 1203.
(40) Kinoshita, K. *Carbon: Electrochemical and Physicochemical Properties*; Wiley: New York, 1988.

Samsung Ex. 1015, Page 5 of 6
Samsung Electronics Co., Ltd., et al. v. Molecular Rebar Design, LLC
IPR2025-00355

Conclusions

The oxidative functionalization of CNTs is important for enhancing chemical activity and depositing metal nanoparticles for heterogeneous catalysis applications. A facile approach to the surface oxidation of CNTs is presented using sonication to promote acidic etching and increase the population density of surface oxide groups. During the CNT surface oxidation, some —C=O was formed along with —C—O—, with the latter taking up the greater population and hence likely playing a dominant role in the tethering of the CNTs, rendering them suitable for nanoparticle decoration for applications in catalysis. In addition to these surface functional groups, adsorbed H_2O is present (likely originating from the aqueous solvent used in preparing the CNTs), and there is evidence for adsorbed —CO. Uptake plots with the C 1s coverage as determined by the C 1s and O 1s core levels also show a sonochemical saturation at 4 h with most of the oxidation occurring by 2 h. This relatively short time for CNT oxidation/ functionalization is desirable for minimizing structural damage to the CNTs that could lead to changes in their properties. Faster settling in ethanol was attributed to fewer and weaker interactions between the CNTs and the solvent molecules. The enhanced electrochemical activities were clearly shown in the CVs due to redox reactions of the surface oxide. By and large, the reactivity of the —C—O—/—C=O groups plays a role. The double layer capacitance of the sonochemically treated CNTs increases with a longer treatment time. The peak currents of the redox reactions of the surface oxides clearly showed a leveling off after a 4-h sonochemical treatment. This saturation was attributed to insufficient sonication power.

Acknowledgment. We acknowledge with pleasure the support of this work by the University of Missouri—Rolla, the Missouri Research Board, and (in part) the American Chemical Society Petroleum Research Fund (39542-G2).

LA047268E

Samsung Ex. 1015, Page 6 of 6
Samsung Electronics Co., Ltd., et al. v. Molecular Rebar Design, LLC
IPR2025-00355